



Removal of anionic dye from aqueous solution using magnetic sodium alginate beads

M.A. El-Bindary ^{1*}, I.M. El-Deen ², A.F. Shoair ³

¹Chemical Engineering Department, Higher Institute of Engineering and Technology, Damietta, Egypt

²Chemistry Department, Faculty of Science, University of Port Said, Port Said, Egypt

³Chemistry Department, Faculty of Science, University of Damietta, Damietta, Egypt

Received 27 June 2019,
Revised 31 July 2019,
Accepted 01 Aug 2019

Keywords

- ✓ Adsorption,
- ✓ Magnetic beads,
- ✓ Kinetics,
- ✓ Thermodynamics.

m.a_bindary@yahoo.com ;
Phone: +2 01146126591

Abstract

Magnetic sodium alginate beads (MSAB) was synthesized and used for the adsorption of hazardous azo pyrazole dye (AP). The effect of different variables in the batch method as a function of solution pH, contact time, concentration of adsorbate, adsorbent dosage and temperature were investigated and optimal experimental conditions were ascertain. Surface modification of MSAB using scanning electron microscopy (SEM) was obtained. More than 80 % removal efficiency was obtained within 70 min. at adsorbent dose of 0.02 g for initial dye concentration of 4×10^{-5} – 1×10^{-3} M at pH 2. The Brunauer-Emmett-Teller (BET) surface area and Barrett-Joyner-Halenda (BJH) pore volume were calculated and found to be $111.061 \text{ m}^2\text{g}^{-1}$ and $0.148 \text{ cm}^3\text{g}^{-1}$, respectively. The point of zero charge (pH_{PZC}) of MCAB was determined and found to be 7.5. The molecular and electronic structure of the investigated dye was also studied using quantum chemical calculations. The adsorption equilibrium showed that the Langmuir equation represented best fit of the experimental data than others. The adsorption kinetics was found to follow pseudo-second-order kinetic model, suggesting a chemisorption process. Adsorption thermodynamics study suggested that the adsorption reactions were spontaneous, endothermic and thermodynamically favorable.

1. Introduction

Organic dyes are widely used in various fields and seriously induce water pollution. Most of the industrial dyes are toxic, carcinogenic, and teratogenic [1] and unfortunately most of them are stable and resistance to photo degradation, biodegradation, oxidizing agents [2]. Conventional physicochemical and biological treatment methods are ineffective for removal these dyes due to their extreme stability. Hence, adsorption technique becomes one of the preferable choices to purify the waste water which containing dyes. In fact, 60-70% of all dyes stuff in use and production fall in this group [3]. According to a statistical data survey, one million tons of such dyes are produced annually worldwide. It can simply be defined as any class of artificial dyes that contains the azo group ($-\text{N}=\text{N}-$). When describing a dye molecule, nucleophiles are referred to as auxochromes, while the aromatic groups are called chromophores. Together, the dye molecule is often described as a chromogen [4]. Synthesis of most azo dyes involves diazotization of a primary aromatic amine, followed by coupling with one or more nucleophiles.

The industrial wastewater usually contains a variety of organic compounds and toxic pulp mills and dyestuff manufacturing discharge highly colored wastewater which has provoked serious environmental concerns all over the world. Several methods including adsorption, coagulation, membrane filtration and advanced oxidation [5], [6] have been employed to eliminate dyes from wastewaters. Among them, adsorption has been recognized as a promising technique due to its high efficiency, simplicity of design, ease of operation as well as the wide suitability for diverse types of dyes. Because the dye effluent may cause damage to aquatic biota and human by mutagenic and carcinogenic effects, the removal of dye pollutants from wastewater is of great importance [7].

Alginate is a natural polysaccharide extracted from brown seaweed. It has many advantages such as availability, low cost, non-toxicity, biocompatibility and biodegradability, and is also an efficient biosorbent due to the presence of carboxylate functions along its chains. Recently, composite sorbents like calcium alginate beads have attracted some attention because they combine the properties and advantages of each of their components [8]. The adsorption properties of the sodium alginate beads containing magnetic nanoparticles in this study are assessed by using organic dye as model of pollutant: negatively charged azo pyrazole dye. Such dyes are also pollutants themselves: used in a lot of industries (textile, paper, food, etc.), their presence in the effluents reduces light penetration and photosynthesis, while some dyes prove toxic or carcinogenic: this makes their removal an important challenge.

Present study was designed to appraise the efficiency of magnetic sodium alginate beads as adsorbent for removal of hazardous azopyrazole dye from aqueous solution. Experimental parameters affecting the adsorption process such as initial adsorbate concentration, adsorbent dosage, contact time, solution pH and temperature were studied. The optimized bond lengths, bond angles and quantum chemical parameters of AP were calculated. The experimental equilibrium adsorption data was analyzed by kinetic and isotherm models. The thermodynamics of the adsorption indicated spontaneous and endothermic nature of the process.

2. Materials and methods

2.1. Physical measurements

C, H and N were determined on Automatic Analyzer CHNS Vario ELIII, Germany. Spectroscopic data of the investigated dye were obtained using the following instruments: FT-IR spectra (KBr discs, 4000-400 cm^{-1}) by Jasco-4100 spectrophotometer; the ^1H NMR spectrum by Bruker WP 300 MHz using DMSO- d_6 as a solvent containing TMS as the internal standard; Mass spectrum by Shimadzu GC-MS-QP2010 Plus instrument. The SEM results of the MSAB sample before and after the adsorption processes were obtained using (JEOL-JSM-6510 LV) scanning microscope to observe surface modification. UV-visible spectrophotometer (Perkin-Elmer AA800 Model AAS) was employed for absorbance measurements of samples. An Orion 900S2 model digital pH meter and a Gallenkamp Orbital Incubator were used for pH adjustment and shaking, respectively. N_2 adsorption/desorption isotherms on MSAB at 77 K was measured on a Quantachrome Nova Instruments version 10, from which the Brunauer-Emmett-Teller (BET) surface area and Barrett-Joyner-Halenda (BJH) pore volume were calculated. The molecular structures of the investigated dye (AP) were optimized by HF method with 3-21G basis set. The molecule was built with the Perkin Elmer ChemBio Draw and optimized using Perkin Elmer ChemBio3D software [9].

2.2. Azopyrazole dye (AP):

The azo compound of 3-(2-hydroxy-5-(4-sulphonic acid phenylazo))-5-phenyl-4,5-dihydro-1H-pyrazole (AP) was prepared previously [10]. The investigated dye (AP) characteristics and its chemical structure is shown in Table 1.

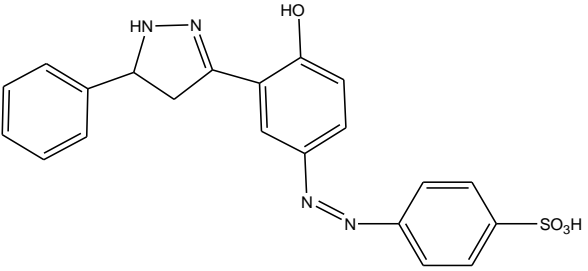
2.2. Preparation of magnetic sodium alginate beads

Magnetic sodium alginate beads (MSAB) was prepared by precipitation of FeSO_4 and FeCl_3 in alkaline solution in the presence of sodium alginate. In a beaker, 25 mL of ammonium hydroxide solution was mixed with 15 mL of deionized water to obtain an alkaline solution. In another beaker, 9.36 g FeCl_3 and 3.44 g FeSO_4 were dissolved in 100 mL deionized water and then added to 40 mL of sodium alginate aqueous solution (2%, w/w) at room temperature for 2 hr with stirring. The obtained black precipitate was separated in a magnetic field and washed with deionized water. Finally, MSAB particles were dried at 80°C. The coating of particles may occur by electrostatic attraction between carboxylate groups of sodium Alginate, Fe^{2+} and Fe^{3+} ions of Fe_3O_4 particles. MSAB was characterized by FTIR and X-ray diffraction measurement (XRD). FTIR (KBr) ($\nu \text{ cm}^{-1}$): 3390 (OH), 1610 (COO)_{asym}, 1410 (COO)_{sym}, 580, 460 (Fe-O), 1095, 1035 (C-O); XRD, diffraction peaks of (220), (311), (400), (422), (511), and (440). Also, the surface area, pore volume and the point of zero charge were calculated.

2.3. Determination of point of zero charge

The point of zero charge (pH_{PZC}) was determined by solid addition method [11]. A series of 0.1 M KNO_3 solutions (50 mL each) were prepared and their pH values were adjusted in the range of 1.0 to 12.0 by addition of 0.1 mol.L^{-1} HCl and 0.1 mol.L^{-1} NaOH. To each solution, 0.1 g of MSAB was added and the suspensions were shaken manually and the solution was kept for a period of 48 h with intermittent manual shaking. The final pH of the solution was recorded and the difference between initial and final pH (ΔpH) (Y-axis) was plotted against the initial pH (X-axis). The point of this curve yielded pH_{PZC} .

Table 1: Properties of the adsorbate (AP) used in the study.

<i>Parameter</i>	<i>Citrullus Colocynthis (%)</i>
<i>Chemical name</i>	3-(2-hydroxy-5-(4-sulphonic acid phenylazo))-5-phenyl-4,5-dihydro-1H-pyrazole
<i>Type color</i>	Anionic
<i>Chemical formula</i>	C₂₁H₁₈N₄O₄S
<i>Molecular weight (g/mol)</i>	422.47
<i>Wavelength of maximum absorption (nm)</i>	437
<i>Molar extinction coefficient, ε₄₃₇ (M⁻¹ cm⁻¹)</i>	2000
<i>Chemical structure of color</i>	

2.4. Batch adsorption experiments

Batch adsorption studies were carried out by shaking 50 mL conical flasks containing 0.02 g of (MSAB) and 25 mL of dye solutions of desired concentration with adjusted pH on an orbital shaker machine at 200 rpm at 25 °C. The solution pH was adjusted with 0.1 mol.L⁻¹ HCl and 0.1 mol.L⁻¹ NaOH solutions. At the end of the adsorption period, the supernatant solution was separated magnetically. Then the concentration of the residual dye was determined spectrophotometrically by monitoring the absorbance at 437 nm for dye using UV–Vis spectrophotometer. Percentage of dye removal (R) was calculated using Eq. (1):

$$R = 100 (C_0 - C_t) / C_0 \quad (1)$$

where C₀ (mmol.g⁻¹) and C_t (mmol.g⁻¹) are dye concentration initially and at time t, respectively. For adsorption isotherms, dye solutions different concentrations (4x10⁻⁵–1x10⁻³M) were agitated with known amounts of adsorbents until the equilibrium was achieved. Equilibrium adsorption capacity, q_e (mmol dye per g adsorbent) was calculated from the following Eq. (2):

$$q_e = V (C_0 - C_t) / W \quad (2)$$

where C_t (mmol.g⁻¹) is the dye concentration at equilibrium, V (L) is the volume of solution and W (g) is the weight of adsorbent.

The procedures of kinetic experiments were identical with those of equilibrium tests. At predetermined moments, aqueous samples (5 mL) were taken from the solution, the liquid was separated from the adsorbent magnetically and concentration of dye in solution was determined spectrophotometrically at a wavelength of 437 nm. The amount of dye adsorbed at time t, q_t (mmol.g⁻¹) was calculated by following Eq. (3):

$$q_t = V (C_0 - C_t) / m \quad (3)$$

where C₀ (mmol.g⁻¹) is the initial dye concentration, C_t (mmol.g⁻¹) the dye concentration at any time t, V (L) the volume of the solution and m (g) is the mass of the adsorbent.

The amount of the dye adsorbed onto (MSAB) at equilibrium and at different temperatures 20, 25, 30, 35, 45 °C, have been examined to obtain thermodynamic parameters for the adsorption system.

3. Results and discussion

3.1. Molecular structure of AP

The atomic numbering and molecular structures (HOMO & LUMO) of AP are calculated and presented in Fig. 1. The HOMO–LUMO energy gap, ΔE, which is an important stability index, is applied to develop theoretical models for explaining the structure and conformation barriers in many molecular systems. The smaller value of ΔE is the more stability the compound [12]. The calculated quantum chemical parameters are given in Table 2. Additional parameters such as separation energies, ΔE, absolute electro negativities, χ, chemical potentials, Pi, absolute hardness, η, absolute softness, σ, global electrophilicity, ω, global softness, S, and additional electronic charge, ΔN_{max}, have been calculated according to the following Eqs. (4–11):

$$\Delta E = E_{LUMO} - E_{HOMO} \quad (4)$$

$$\chi = \frac{-(E_{HOMO} + E_{LUMO})}{2} \quad (5)$$

$$\eta = \frac{E_{LUMO} - E_{HOMO}}{2} \quad (6)$$

$$\sigma = 1/\eta \quad (7)$$

$$Pi = -\chi \quad (8)$$

$$S = \frac{1}{2\eta} \quad (9)$$

$$\omega = Pi^2 / 2\eta \quad (10)$$

$$\Delta N_{max} = -Pi / \eta \quad (11)$$

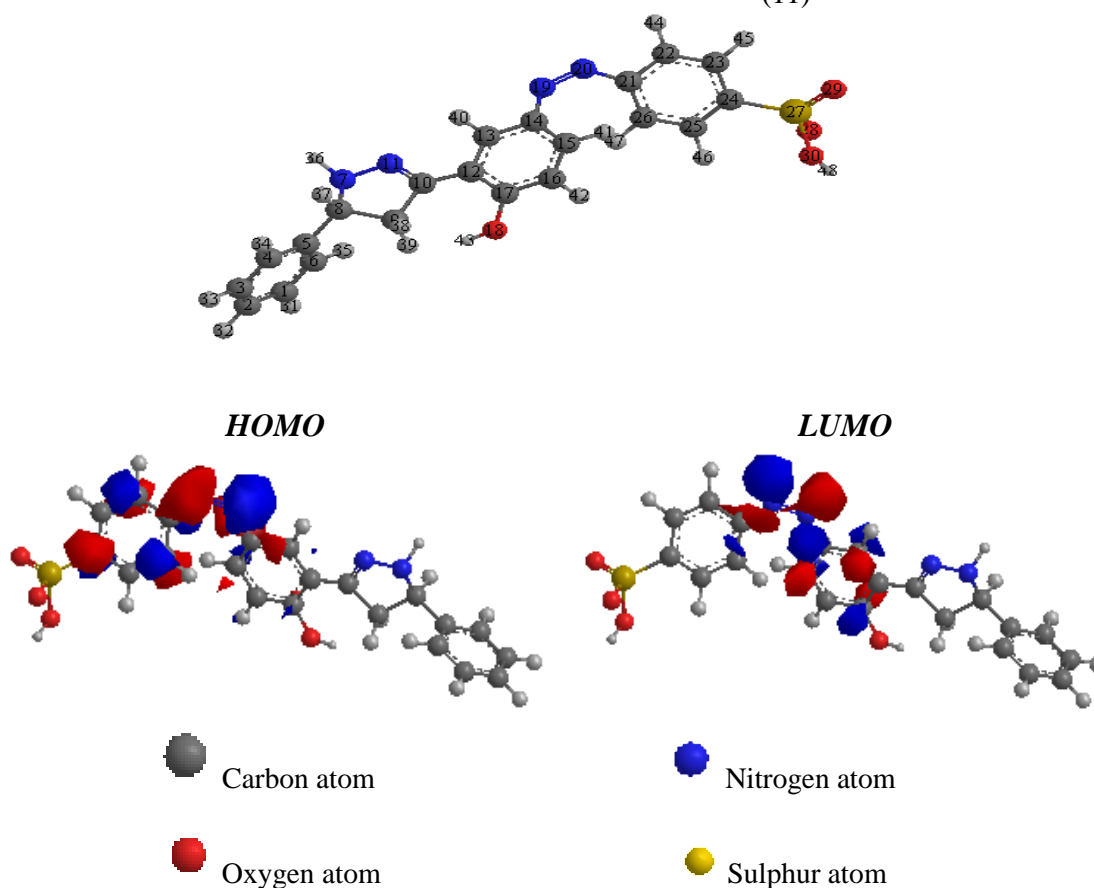


Figure 1: The molecular structure (HOMO & LUMO) of AP.

Table 2: The calculated quantum chemical parameters of AP.

E_{HOMO} (eV)	E_{LUMO} (eV)	ΔE (eV)	χ (eV)	η (eV)	σ (eV ⁻¹)	Pi (eV)	S (eV ⁻¹)	ω (eV)	ΔN_{max}
-4.117	-3.559	0.558	3.838	0.279	3.58423	-3.838	0.1395	1.919	13.75627

3.2. Brunauer-Emmett-Teller (BET) surface area.

The Brunauer-Emmett-Teller (BET) [13] surface area and Barrett-Joyner-Halenda (BJH) pore size of MSAB have been investigated using N₂ adsorption/desorption measurements at 77 K. The adsorption isotherm is classified as type IV according to IUPAC exhibiting an H1 hysteresis loop that closes at P/P₀=0.987. This type of hysteresis which contains two branches that almost vertical and nearly over an appreciable range of gas uptake arises from the existence of cylindrical pores open at both ends. The specific surface area (A_{BET}) of the prepared sample (MSAB) is 111 m²/g which was estimated by using the BET equation in its normal range of applicability

and adopting a value of 16.2 Å for the cross-sectional area of N₂. However, the total pore volume (V_p) taken at a saturation pressure and expressed as liquid volume = 0.148 cm³/g and the average pore radius = 26.6 Å. Porosity detection is accomplished by constructing the V_a-t plot in which the reference value of statistical thickness, t, are those of Lecloux and Pirard which fulfilled the criteria for their proper choice based on BET C-constant. The t-curve of the prepared solid shows an upward deviation revealing the mesoporosity of sample. The closure point of the hysteresis loop of the adsorption isotherm agrees with the starting point of the upward deviation. The pore size distributions of the samples were assessed by the Barret, Joyner, and Halenda (BJH) method and formed two peaks, the first one is centered at 13.3 Å that belongs to super micropores and the second one is broad centered at 18.6 Å reveals a sample mesoporosity.

3.3. Determination of point of zero charge (pH_{PZC})

pH was one of the most important parameters for AP sorption, as it determined which ionic species were present in the adsorbate solution and the surface charge of the sorbent. Surface charge of the MSAB was determined by the PZC, which is defined as the pH (pH_{PZC}) at which the positive charges on the surface equal the negative charges [14]. The pH_{PZC} of MSAB was found to be 7.5. This shows that below this pH, the MSAB acquires a positive charge due to protonation of functional groups and above this pH, negative charge exists on the surface of MSAB. The adsorption of anionic dyes is favored at pH < pH_{PZC} where the surface becomes positively charged.

3.4. SEM analysis

Scanning electron microscopy (SEM) has been a primary tool for characterizing the surface morphology and fundamental physical properties of the adsorbent surface. It is useful for determining the particle shape, porosity and appropriate size distribution of the adsorbent. Raw MSAB has considerable numbers of pores where, there is a good possibility for dyes to be trapped and adsorbed into these pores. MSAB adsorbed with tested dye show very distinguished dark spots which can be taken as a sign for effective adsorption of azopyrazole dye molecules in the cavities and pores of this adsorbent [15].

3.5. Effect of pH

The pH value of aqueous solution is an important parameter in the adsorption study of anionic dyes because of its effect on both ionization of dye molecules and surface binding sites. The removal of the tested dye (AP) by MSAB at different pH values (1–10) was studied at initial concentrations of 1 × 10⁻³ M of the dye, 25 °C and 0.02 g adsorbent dosage. MSAB has proved to be an effective adsorbent for the removal of the dye and the most effective pH was 2 and it was used in further studies (Fig. 2). The investigated dye was of anionic in nature, so they release colored dye anion on dissolution. The percentage of color removal decreased when the pH increased from 2 to 9. It may be considered for two possible mechanism of adsorption of dye on the adsorbent: (i) electrostatic interaction between the adsorbent and the dye molecule, (ii) a chemical reaction between the dye and the adsorbent. At pH 2, the concentration of H⁺ ion increased and the adsorbent surface acquires positive charge by absorbing H⁺ ions. As the adsorbent surface is positively charged at low pH, there may be a high electrostatic attraction exists between the positively charged surface of the adsorbent and the anionic dye molecule, a maximum dye adsorption takes place. The experimental determination of pH_{PZC} of MSAB revealed that this composite has pH_{PZC} 7.5. As the pH of the system increases, the number of negatively charged sites increases and the number of positively charged sites decreases. Negatively charged surface sites on the adsorbent surface do not favor the adsorption, due to the electrostatic repulsion. Also lower adsorption of the selected anionic dye at alkaline pH is due to the presence of excess -OH ions, which destabilize anionic dye and compete with the dye anions for the adsorption sites.

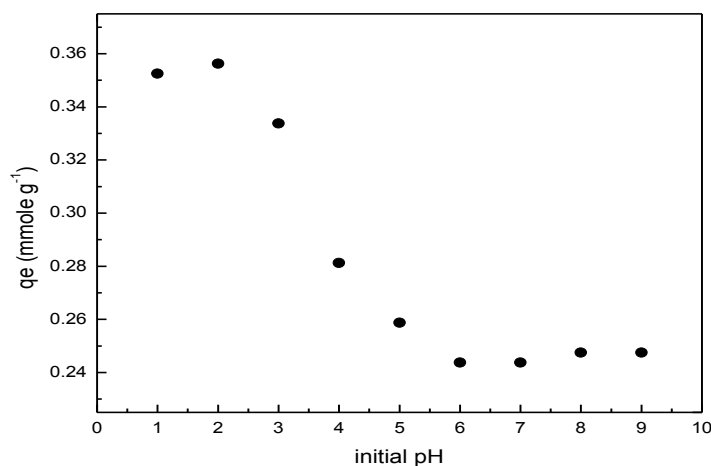


Figure 2: pH effect on AP adsorption using the adsorbent (MSAB): (T: 25 °C; C₀: 1x10⁻³ M).

3.6. Effect of adsorbent dosage

The uptake of dye with change in adsorbent dosage (0.01–0.1 g) at adsorbate concentrations of 2x10⁻⁴ M at 25 °C and pH 2 was tested. Adsorption of dye shows that the uptake of dye per gram of adsorbent increases with increasing adsorbent dosage from 0.01 to 0.1 g. The increase in adsorbent dose, did not cause any significant increase in % removal of dye. This was due to the concentration of AP reached at equilibrium status between solid and solution phase. The dye removal increased up to a certain limit and then it remains almost constant in all the cases. This was due to the availability of more adsorbent sites and high specific surfaces of the adsorbents. The decrease in amount of dye adsorbed q_e (mmol.g⁻¹) with increasing adsorbent mass is due to the separation of the concentration gradient between solute concentration in the solution and the solute concentration in the surface of the adsorbent.

3.7. Effect of contact time

The AP removal increases with time and attains saturation in about 5-90 mins. Basically, the removal of adsorbate is rapid, but it gradually decreases with time until it reaches equilibrium. The AP dye showed a fast rate of sorption during the first 60 mins of the adsorbate/adsorbent contact and the rate of amount removal becomes almost insignificant due to a quick exhaustion of the adsorption site. The rate of amount dye removal is higher in the beginning due to a larger surface area of the adsorbent being available for the dye adsorption.

3.8. Effect initial concentration (C₀)

The removal of azopyrazole dye (AP) by adsorption on the adsorbent (MSAB) was shown to increase with time and attained a maximum value at about 70 mins, and thereafter, it remained almost constant. On changing the initial concentration of dye solution from 4x10⁻⁵–3x10⁻³ M at 25 °C, pH 2 and 0.02 g adsorbent dosage the amount of removed dyes was decreased. It was clear that the removal of the dye was dependent on the initial concentration of the dye because the decrease in the initial dye concentration increased the amount of dye adsorbed. This is very clear because, for a fixed adsorbent dose, the number of active adsorption sites to accommodate adsorbate ions remains unchanged but with increasing adsorbate concentration, the adsorbate ions to be accommodated increases and hence the percentage of adsorption goes down. At higher concentrations, lower removal percentage was observed because of the saturation of the adsorption sites.

3.9. Effect of temperature

Temperature dependence of the adsorption process is associated with several thermodynamic parameters. The plot of amount of adsorbate per amount of adsorbent of adsorption as a function of temperature shows a small increasing trend with rise in temperature from 20 to about 45 °C. Equilibrium capacity can be changed by temperature of the adsorbent for a particular adsorbate. In our case the experimental data obtained at pH 2, adsorbent dosage 0.02 g, and initial concentration of 2x10⁻⁴ M show that increase in the adsorption capacity at temperature from 20 to 45 °C.

3.10. Adsorption isotherms

Isotherm studies give significant insights by clarifying the adsorbate distribution between solid and solution phase during the adsorption equilibrium, and adsorption isotherms reveal the behavior of adsorbate how to interact with adsorbent. Equilibrium studies that give the capacity of the adsorbent and adsorbate are described by adsorption isotherms, which is usually the ratio between the quantity adsorbed and that remained in solution at equilibrium at fixed temperature. Various isotherm models have been used for considering the equilibrium adsorption of compounds from solutions such as Langmuir [16], [17], Freundlich [18], Dubinin–Radushkevich [19] and Temkin [20]. The Langmuir isotherm model assumes the uniform energies of adsorption onto the adsorbent surface. It is based on assumption of the existence of monolayer adsorption onto a completely homogeneous surface with a finite number of identical sites and with negligible interaction between adsorbed molecules [17]. The Freundlich model is an empirical equation based on adsorption of heterogeneous surface or surface supporting sites of varied affinities. It is assumed that the stronger binding sites are occupied first and that the binding strength decreases with the increasing degree of site occupation [18]. Dubinin–Radushkevich isotherm is an empirical model initially for the adsorption of subcritical vapors onto micropore solids following a pore filling mechanism. It is applied to distinguish the physical and chemical adsorption for removing a molecule from its location in the sorption space to the infinity [19]. The Temkin isotherm assumes that the heat of adsorption of all molecules in the phase decreases linearly when the layer is covered and that the adsorption has a maximum energy distribution of uniform bond [20].

The linear and nonlinear forms of Langmuir, Freundlich, Dubinin–Radushkevich and Temkin isotherm models and their parameters are shown in Table 3, where q_e the adsorbed amount of dye at equilibrium concentration (mmol.g^{-1}), q_m is the maximum sorption capacity (corresponding to the saturation of the monolayer, mmol.g^{-1}) and K_L is the Langmuir binding constant which is related to the energy of sorption (L.mmol^{-1}), C_e is the equilibrium concentration of AP dye in solution (M). K_F (mmol.g^{-1}) (L.mmol^{-1}) $^{1/n}$ and n are the Freundlich constants related to the sorption capacity and intensity, respectively. K_{DR} ($\text{J}^2 \text{mol}^{-2}$) is a constant related to the sorption energy, Q_{DR} (mmol.g^{-1}) is the theoretical saturation capacity, ϵ ($\text{J}^2 \text{mol}^{-2}$) is the Polanyi potential. R ($8.314 \text{ Jmol}^{-1}\text{K}^{-1}$) is the gas constant, T is the temperature where the adsorption occurs, K_T (L.mmol^{-1}) is the Temkin isotherm constant, β_T (J.mol^{-1}) is Temkin constant in relation to heat of adsorption.

Table 3. Isotherms and their linear forms for the adsorption of AP onto MSAB.

Isotherm	Equation	Value of parameters	
Langmuir	$\frac{C_e}{q_e} = \frac{1}{q_m K_L} + \frac{C_e}{q_m}$ <p>The constants q_m and K_L are calculated by the plot of C_e/q_e vs. C_e with slope $1/q_m$ and intercept $1/(q_m K_L)$</p>	$q_{m\text{exp}}$ (mmole g^{-1})	0.1875
		q_m (mmole g^{-1})	0.19925
		K_L (L mg^{-1})	90438.7825
		R^2	0.99
		n	2.627707
Freundlich	$\ln q_e = \ln K_F + \frac{1}{n} \ln C_e$ <p>K_F and n can be calculated from a linear plot of $\ln q_e$ vs. $\ln C_e$</p>	K_F (L mg^{-1})	1.85255
		R^2	0.85324
		Q_{DR}	-0.15606
Dubinin–Radushkevich	$\ln q_e = \ln Q_{DR} - K_{DR} \epsilon^2$ <p>The slope of the plot of $\ln q_e$ vs. ϵ^2 gives K_{DR} ($\text{mol}^2 (\text{kJ}^2)^{-1}$) and the intercept yields the adsorption capacity, Q_{DR} (mg g^{-1})</p>	K_{DR}	-2.878E-09
		E_a	16.75
		R^2	0.8941
		β_T	71051.68
Temkin	$q_e = \beta_T \ln K_T + \beta_T \ln C_e$ <p>The parameters β and K_T are the Temkin constants that can be determined by the plot of q_e vs. $\ln C_e$</p>	K_T (L mg^{-1})	14.3146
		R^2	0.86118

The Langmuir isotherm model was found to be the most suitable model for describing the isotherm for the adsorption of the AP dye into the MSAB sorbent (Fig. 3). However, from the isotherm fitting, the Freundlich lines deviated from the experimental data points. The isotherm fitting was plotted on the basis of the nonlinear equations using the model constant parameters obtained from the linear equation plot analysis. The Langmuir

model presented the high correlation coefficient $R^2= 0.995$) may giving an indication that chemisorptions (Evidenced by kinetic studies). In addition, the q_m calculated from the Langmuir isotherm was close to the experimental q_{max} . Analysis of isotherm parameters proposed by Dubinin-Radushkevich were calculated (Table 3). This isotherm was developed taking into account the effect of the porous structure of the sorbent, and the energy involved in the sorption process. The results of Dubinin-Radushkevich isotherm are reported in Table 3 and Fig. 4. The value of the mean energy of sorption is $16.75 \text{ kJ.mol}^{-1}$: this is consistent with the proposed mechanism of chemisorption. Indeed, it is generally admitted that 8 kJ.mol^{-1} is the limit energy for distinguishing, physical (below 8 kJ.mol^{-1}) and chemical sorption (up 8 kJ.mol^{-1}).

A comparison of the correlation coefficient values obtained from the Langmuir, Freundlich, Dubinin-Radushkevich and Temkin isotherm models (Table 3), reveals that the correlation coefficients for the Langmuir isotherm are higher than those for the Freundlich, Dubinin-Radushkevich and Temkin isotherm models. This result suggests that the binding of dye ions may occur as a monolayer on the surface of the sorbent and that the uptake occurs on a homogenous surface by monolayer sorption. This should be confirmed by experimental observation for confirmation. The uptake can be described in terms of chemisorption as ion exchange mechanism.

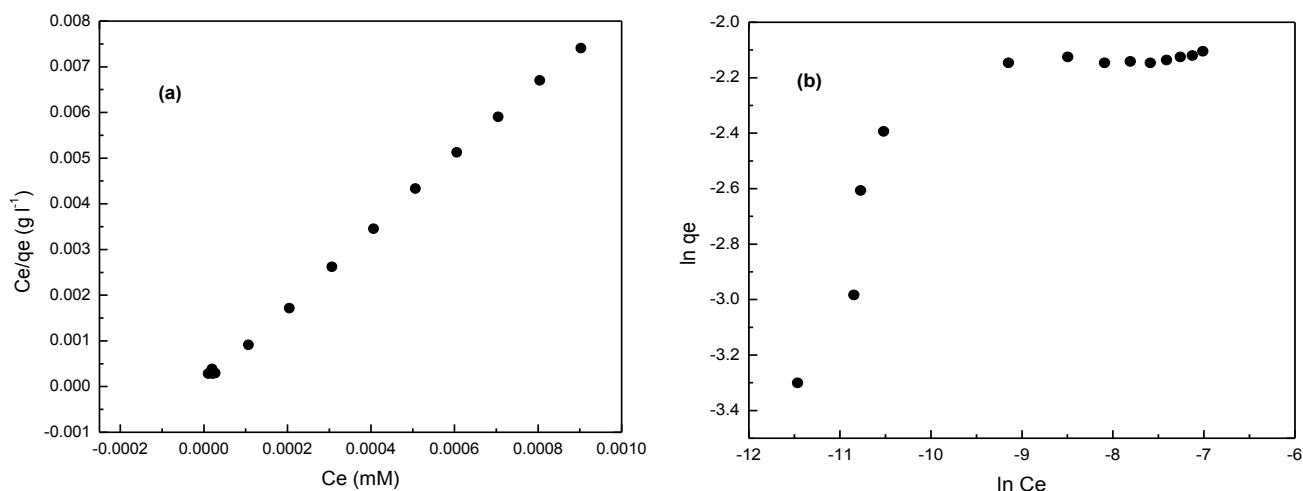


Figure 3: Linearized plots for sorption isotherms:(a) Langmuir equation, (b) Freundlich equation.

The presence the same type of functional groups is comforting the hypothesis of homogeneous surface (or homogeneous energies of sorption). The ranking of the models as follow: Langmuir > Dubinin-Radushkevich > Temkin > Freundlich.

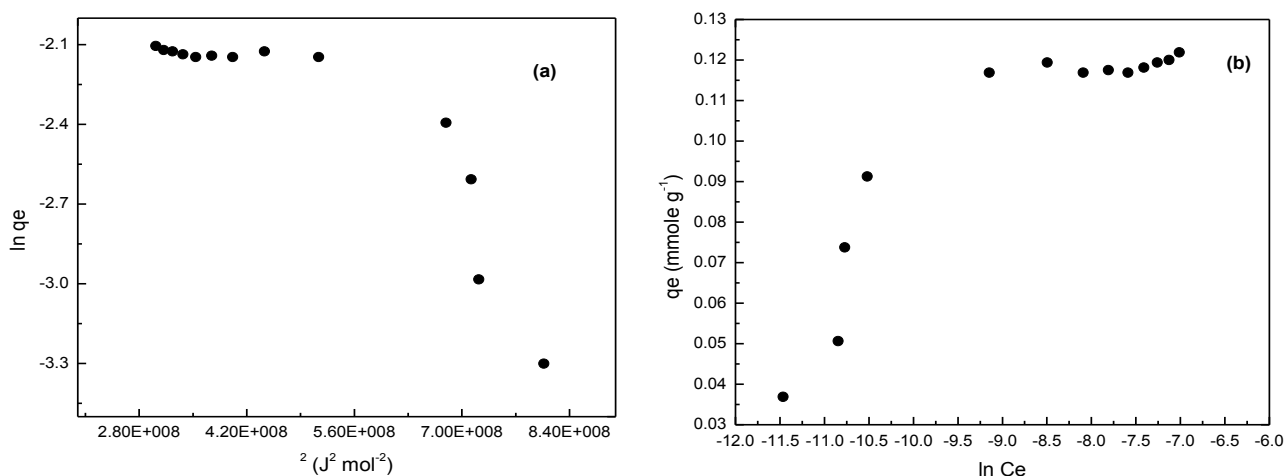


Figure 4: Linearized plots for sorption isotherms: (a) Dubinin–Radushkevich equation, (b) Temkin model.

3.11. Adsorption kinetics and mechanism studies

The study of adsorption kinetics describes the solute uptake rate and evidently this rate controls the residence time of adsorbate uptake at the solid-solution interface. The rate of removal of tested dye by adsorption was rapid initially and then slowed gradually until it attained an equilibrium beyond which there was significant increase in the rate of removal. The maximum adsorption was observed at 70 min. and it is thus fixed as the equilibrium time.

Aiming at evaluating the adsorption kinetics of tested dye onto MSAB, the pseudo-first-order and pseudo-second-order kinetic models were used to fit the experimental data, according to the below kinetic model equations. The pseudo-first-order rate expression of Lagergren [21] is given as:

$$\log (q_e - q_t) = \log q_e - k_1 t \quad (12)$$

The pseudo-second-order kinetic model [22] is expressed as:

$$t/q_t = 1/k_2 q_2^2 + 1/q_2 t \quad (13)$$

where q_t is the amount of dye adsorbed (mmol.g^{-1}) at various times t , q_e is the maximum adsorption capacity (mmol.g^{-1}) for pseudo-first-order adsorption, k_1 is the pseudo-first-order rate constant for the adsorption process (min^{-1}), q_2 is the maximum adsorption capacity (mmol.g^{-1}) for the pseudo-second-order adsorption, k_2 is the rate constant of pseudo-second-order adsorption ($\text{gmol}^{-1}\text{min}^{-1}$). The straight-line plots of $\log (q_e - q_t)$ vs. t for the pseudo-first-order reaction and t/q_t vs. t for the pseudo-second-order reaction (Fig. 5) for the adsorption of tested dye onto (MSAB) have also been tested to obtain the rate parameters. The k_1 , k_2 , q_e , q_2 , and correlation coefficients, r_1^2 and r_2^2 for the dye under different temperatures were calculated from these plots and are given in Table 4.

Since neither the pseudo-first-order nor the pseudo-second-order model can identify the diffusion mechanism, the kinetic results were further analyzed for diffusion mechanism by using the intra-particle diffusion model. The effect of intra-particle diffusion constant (internal surface and pore diffusion) on adsorption can be determined by the following equation.

$$q_t = k_{id} t^{1/2} + I \quad (14)$$

where I is the intercept and k_{id} is the rate constant of intra-particle diffusion ($\text{mg.g}^{-1}.\text{h}^{-1/2}$) which is determined from the linear plot of q_t vs. $t^{1/2}$ (Fig. 6), and it is usually used to compare mass transfer rates. According to this model, the plot of uptake, q_t , vs. the square root of time, $t^{1/2}$ should be linear if intra-particle diffusion is involved in the adsorption process and if these lines pass through the origin, then intra-particle diffusion is the rate controlling step. The intra-particle diffusion rate constant and intercept values are displayed in Table 4.

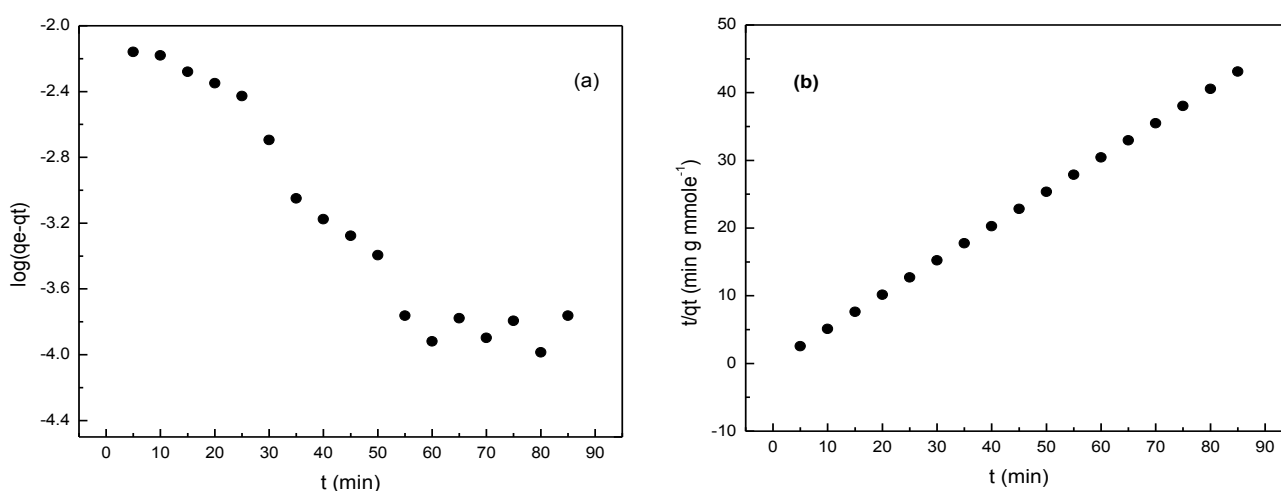


Figure 5: Modeling of uptake kinetics with: (a) pseudo-first-order rate expression, (b) pseudo-second-order rate expression.

Table 4: Kinetic parameters and their correlation coefficients for the adsorption of AP onto MSAB.

Model	Equation	Value of parameters
<i>Pseudo-First-order kinetic</i>	$\log(q_e - q_t)$ $= \log q_e - \left(\frac{K_1}{2.303}\right)t$	<i>The plot of $\ln(q_e - q_t)$ vs. t gives a straight line with the slope $-K_1$ and intercept $\ln q_e$</i>
		$K_1(\text{min}^{-1})$ -0.0259 $q_e (\text{mmole g}^{-1})$ 0.30110 R^2 0.90795
		<i>Values of K_2 and q_e for different initial concentrations of dye were calculated from the slope and intercept of the linear plot of t/q_t vs. t</i>
<i>Pseudo-second-order kinetic</i>	$\frac{t}{q_t} = \frac{1}{K_2 q_e^2} + \frac{t}{q_e}$	$K_2(\text{min}^{-1})$ 12.91180 $q_e (\text{mmole g}^{-1})$ 1.97328 R^2 0.9999
		<i>The parameters K_{dif} and C were determined from the linear plot of q_t vs. $t^{1/2}$</i>
		$K_i (\text{mg g}^{-1} \text{min}^{1/2})$ 0.00109 $X (\text{mg g}^{-1})$ 1.96344 R^2 0.85955
<i>Intraparticle diffusion</i>	$q_t = K_i t^{1/2} + X$	$\beta (\text{g mg}^{-1})$ 336.7 $\alpha (\text{mg g}^{-1} \text{min}^{-1})$ 7.0979 R^2 0.91341
		<i>The constants α and β were obtained from the slope and intercept of a line plot of q_t vs. $\ln t$</i>
		<i>Experimental data</i> $q_e (\text{exp}) (\text{mmole g}^{-1})$ 1.97216

The Elovich equation is used for general application to chemical adsorption [23]. The equation has been applied satisfactorily to some chemical adsorption processes and has been found to cover a wide range of slow adsorption rates. The same equation is often valid for systems in which the adsorbing surface is heterogeneous, and is formulated as:

$$q_t = (1/\beta) \ln(\alpha\beta) + (1/\beta) \ln t \quad (15)$$

Where α is the chemical adsorption rate (mg/mg min) and β is a coefficient in relation with the extension of covered surface and activation energy of chemical adsorption (g/mg). Plot of q_t vs. $\ln t$ gave a linear relationship with slope of $(1/\beta)$ and an intercept of $(1/\beta) \ln(\alpha\beta)$. The $1/\beta$ value reflects the number of sites available for adsorption whereas the value of $(1/\beta) \ln(\alpha\beta)$ indicates the adsorption quantity when $\ln t$ equal to zero.

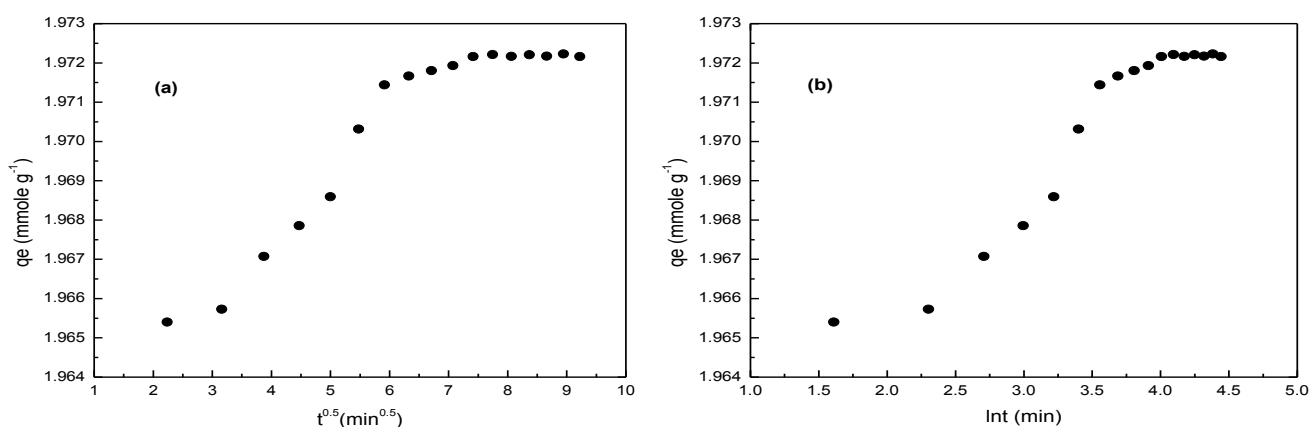


Figure 6: Modeling of uptake kinetics with (a) simplified model of resistance to intraparticle diffusion (Morris and Weber equation), (b) Elovich equation.

Upon comparison among the kinetic models, the R^2 values of the pseudo-second-order kinetic model (0.999) are much higher than those of pseudo-first-order kinetic model (0.907), implying that the kinetics of AP

adsorption follows the pseudo-second-order kinetic model. This consideration is confirmed by the correlation coefficients and the q_e (calc.) value from the pseudo-second-order kinetic model are in good agreement with the experimental results. The rate-limiting step in these adsorption processes may be chemisorption involving strong forces through the sharing or exchanging of electrons between sorbent and sorbate [15]. The intra-particle diffusion curve gives multi linearity, it does not pass through the origin. The intra-particle diffusion kinetic model ($R^2 = 0.859$) was calculated from the slope of the corresponding second linear region (Fig. 6). It is assumed that the external resistance to mass transfer surrounding the particles is significant only in the initial stages of adsorption (initial sharp increase). The second linear portion is the gradual adsorption stage with controlling intraparticle diffusion. When the plots do not pass through the origin, indicates that the pore diffusion is not the sole rate-limiting step but also other kinetic models may control the rate of adsorption, all of which may be operating simultaneously [24]. The Elovich equation assumes that the active sites of the adsorbent are heterogeneous and therefore, exhibit different activation energies for chemisorption. When increasing the concentration of dye, it was observed that the constant α (related to the rate of chemisorption) increased and the constant β (related to the surface coverage) decreased (Table 4), which is due to the decrease in the available adsorption surface for the adsorbates. Therefore, by increasing the concentration, within the range studied, the rate of chemisorption can be increased [25].

Therefore, the adsorption kinetics can be satisfactorily approximated by the pseudo-second-order kinetic model, based on the assumption that the rate-limiting step may be chemisorption involving electrostatic forces through the sharing or exchange of electrons between the adsorbent and the adsorbate.

The adsorption mechanism can be explained by the electrostatic interactions between the negatively charged dye ion and the positively charged sites on the MSAB surface. AP is anionic mono azo dye which contains one sulfonic acid group ($-\text{SO}_3\text{H}$). In aqueous solution the dye dissociates to the hydrogen ions (H^+) and the sulfonate anion ($-\text{SO}_3^-$). At acidic pH, the sulfonic groups can be protonated to the neutral form ($-\text{SO}_3\text{H}$) however, sulfonic groups exhibit negative charge even at higher acidic solutions, due to their pK_a values lower than zero [15]. The surface of MSAB contain some oxygen groups such as carboxylic groups ($-\text{COOH}$) and hydroxylic groups ($-\text{OH}$). At basic pH the carboxylic and hydroxylic groups are deprotonated to anionic form ($-\text{COO}^-$ and $-\text{O}^-$) and generates electrostatic repulsion force with dye anions. Therefore, the adsorption capacity of AP onto MSAB is quite low in basic media. At acidic pH, carboxylic and hydroxylic groups are protonated to the cationic form ($-\text{COOH}_2^+$ and $-\text{OH}_2^+$) [25]. Thus, when the pH of the dye solution decreases, the number of negatively charged sites on MSAB decreases and the number of positively charged sites increases which favor the adsorption of negatively charged dye ions because of the electrostatic force of attraction. Therefore, the adsorption capacity of AP onto MSAB surface is more favorable at lower pH.

3.12. Thermodynamic parameters

The thermodynamic parameters reflect the feasibility and spontaneous nature of the adsorption process. Values of thermodynamic parameters are the actual indicators for practical application of a process. The amount of the dye adsorbed onto (MSAB) at equilibrium and at different temperatures 20, 25, 30, 35, 45 °C, have been examined to obtain thermodynamic parameters for the adsorption system. The pseudo-second-order rate constant of tested dye adsorption is expressed as a function of temperature by the following Arrhenius type relationship [26]:

$$\ln k_2 = \ln A - E_a/RT \quad (16)$$

where E_a is the Arrhenius activation energy of adsorption, A is the Arrhenius factor, R is the gas constant and is equal to $8.314 \text{ J}\cdot\text{mol}^{-1}\text{K}^{-1}$ and T is the operated temperature. A linear plot of $\ln k_2$ vs. $1/T$ for the adsorption was constructed to generate the activation energy from the slope ($-E_a/R$). The chemical (chemisorption) or physical (physisorption) adsorption mechanism are often an important indicator to describe the type of interactions between tested dye and MSAB. The magnitude of activation energy gives an idea about the type of adsorption which is mainly physical or chemical. Low activation energies ($5\text{--}40 \text{ kJ}\cdot\text{mol}^{-1}$) are characteristics for physisorption, while higher activation energies ($40\text{--}800 \text{ kJ}\cdot\text{mol}^{-1}$) suggest chemisorption [27].

The other thermodynamic parameters, change in the standard free energy (ΔG°), enthalpy (ΔH°) and entropy (ΔS°) were determined by using following equations:

$$K_C = C_A/C_S \quad (17)$$

$$\Delta G^\circ = -RT \ln K_C \quad (18)$$

$$\ln K_C = \Delta S^\circ/R - \Delta H^\circ/RT \quad (19)$$

where K_C is the equilibrium constant, C_A is the amount of dye adsorbed on the (MCAB) of the solution at equilibrium ($\text{mmol}\cdot\text{L}^{-1}$), C_S is the equilibrium concentration of the dye in the solution ($\text{mmol}\cdot\text{L}^{-1}$). The q_2 of the

pseudo-second-order model in Table 4 was used to obtain C_A and C_S . T is the solution temperature (K) and R is the gas constant. ΔH° and ΔS° were calculated from the slope and the intercept of van't Hoff plots of $\ln K_C$ vs. $1/T$.

The negative values of the change of free energy (ΔG°) are 8.23, 9.11, 9.99, 10.88 and 12.64 at 20, 25, 30, 35, 45 °C, respectively. These values confirm the feasibility of the adsorption process and also indicate spontaneous adsorption of tested dye onto MCAB in the temperature range studied. The positive value of the standard enthalpy change (ΔH°) is (43.45 kJ.mol⁻¹) indicates that the adsorption is chemical in nature involving strong forces through the sharing or exchanging of electrons between sorbent and sorbate and is also endothermic, thereby demonstrating that the process is stable energetically [28]. The high positive value of standard entropy change (ΔS°) which is (176.41 J.mol⁻¹.K⁻¹) suggests increased randomness at the solid/solution interface with some structural changes in the adsorbate and the adsorbent and an affinity of the adsorbent [29].

3.13. Effect of ionic strength (addition of NaCl)

The effect of chloride ions on AP removal was examined, by addition of increasing concentrations of NaCl (from 10 to 40 g L⁻¹; C_0 : 2×10^{-4} M; sorbent dosage: 0.02 g 25 mL). For the studied adsorbents increasing the amount of NaCl slightly decreases the sorption capacity: the sorption capacity decreases by 20%, when NaCl concentration reaches 20 g.L⁻¹. This is probably due to the competitor effect of chloride anions against AP anions for interaction with the sorption sites. It is noteworthy, that when even NaCl concentration reaches 40 g.L⁻¹ the reduction in the adsorption capacity decreases by 1.5%, this indicates that even under these drastic conditions a high adsorption capacity is maintained.

3.14. Desorption studies

Desorption of anionic dyes is generally operated by pH change. In most cases, desorption is performed under basic conditions. Regeneration of the investigated sorbent (MSAB) was carried by placing 0.02 g of MSAB in the flask and then washed carefully by flowing distilled water. The adsorbent loaded by AP was then subjected for regeneration using 0.1 M NaOH. After regeneration the sorbent was again carefully washed with distilled water to become ready for the second run of uptake [30]. The regeneration efficiency for each adsorption/desorption cycle was found to be 98.6, 96.6, 94.5%. This indicates that Composite has good performance for repeated use up to at least 3 cycles. The efficiency of regeneration was calculated using the following equation:

$$\text{Regeneration efficiency (\%)} = \frac{\text{Total adsorption capacity in the second run}}{\text{Total adsorption capacity in the first run}} \times 100 \quad (20)$$

Sorption/desorption process was carried out for three cycles. Also, the higher efficiency upon reuse suggests recyclability and that basic medium is very suitable in the extraction of the AP from the spent adsorbent.

Conclusion

In conclusion, the magnetic sodium alginate beads (MSAB) is an effective adsorbent for the removal of azopyrazole dye (AP) from aqueous solution. The high adsorption capacity of AP onto MSAB in highly acidic solutions (pH=2) is due to the strong electrostatic interactions between its adsorption site and dye anion. More than 80 % removal efficiency was obtained within 70 min. at adsorbent dose of 0.02 g for initial dye concentration of 4×10^{-5} – 1×10^{-3} M at pH 2. The Brunauer-Emmett-Teller (BET) surface area and Barrett-Joyner-Halenda (BJH) pore volume were calculated and found to be 111.061 m².g⁻¹ and 0.148 cm³.g⁻¹, respectively. The pH_{PZC} of the adsorbent (MSAB) was found to be 7.5. The optimized bond lengths, bond angles and quantum chemical parameters of AP were calculated. For the application of Langmuir, Freundlich, Dubinin–Radushkevich and Temkin adsorption models, the experimental results show that the Langmuir model was the best. The kinetic data tends to fit very well in the pseudo-second-order kinetic model with high correlation coefficients, suggesting a chemisorption process. The activation energy of adsorption was also evaluated and found to be +16.75 kJ.mol⁻¹. The ΔG° values were negative; therefore the adsorption was spontaneous in nature. The positive value of ΔH° reveals that the adsorption process was endothermic in nature. The positive value of ΔS° implies that the increased randomness at the solid/solution interface. Increasing the concentration of NaCl hardly affects the sorption capacity. AP anions can be efficiently desorbed from loaded MSAB with alkaline solution and that sorbent can be reused.

References

1. D.M. Marmion, Handbook of colorant, Wiley, New York, Print ISBN: 9780470511992, Online ISBN: 9780470744970 (1999). [doi: 10.1002/9780470744970](https://doi.org/10.1002/9780470744970).
2. Z. Zhang, J. Kong, Novel magnetic Fe₃O₄@C nanoparticles as adsorbents for removal of organic dyes from aqueous solution, *J. Hazard. Mater.* 193 (2011) 325–329. <https://doi.org/10.1016/j.jhazmat.2011.07.033>
3. W.-K. Li, H.-X. Zhang, Y.-P. Shi, Selective adsorption of aromatic acids by a nanocomposite based on magnetic carboxylic multi-walled carbon nanotubes and novel metal-organic frameworks, *Appl. Surf. Sci.* 416 (2017) 672–680. <https://doi.org/10.1016/j.apsusc.2017.04.202>
4. S. Benkaddour, R. Slimani, H. Hiyane, I. El Ouahab, I. Hachoumi, S. El Antri, S. Lazar, Removal of reactive yellow 145 by adsorption onto treated watermelon seeds: Kinetic and isotherm studies, *Sustain. Chem. Pharm.* 10 (2018) 16–21. <https://doi.org/10.1016/j.scp.2018.08.003>
5. K.Z. Elwakeel, A.A. El-Bindary, E.Y. Kouta, E. Guibal, Functionalization of polyacrylonitrile/Na-Y-zeolite composite with amidoxime groups for the sorption of Cu(II), Cd(II) and Pb(II) metal ions, *Chem. Eng. J.* 332 (2018) 727–736. <http://dx.doi.org/10.1016/j.cej.2017.09.091>
6. Y. Tao, J. Cai, X. Huai, B. Liu, A novel device for hazardous substances degradation based on double-cavitating-jets impingement: Parameters optimization and efficiency assessment, *J. Hazard. Mater.* 335 (2017) 188–196. <https://doi.org/10.1016/j.jhazmat.2017.04.046>
7. A.A. El-Bindary, H.A. Kiwan, A.F. Shoair, A.R. Hawas, A novel crosslinked amphoteric adsorbent thiourea formaldehyde calcium alginate: preparation, characterization and adsorption behaviors of removing color from acidic and basic dyes, *Desalin. Water Treat.* 151 (2019) 145–160. [doi: 10.5004/dwt.2019.23809](https://doi.org/10.5004/dwt.2019.23809)
8. R. Rostamian, H. Behnejad, A comprehensive adsorption study and modeling of antibiotics as a pharmaceutical waste by graphene oxide nanosheets, *Ecotoxicol. Environ. Safety* 147 (2018) 117–123. [doi: 10.1016/j.ecoenv.2017.08.019](https://doi.org/10.1016/j.ecoenv.2017.08.019)
9. A.F. Shoair, A.A. El-Bindary, N.A. El-Ghamaz, G.N. Rezk, Synthesis, characterization, DNA binding and antitumor activities of Cu(II) complexes, *J. Mol. Liq.* 269 (2018) 619–638. <https://doi.org/10.1016/j.molliq.2018.08.075>
10. I.M. El-Deen, A.F. Shoair, M.A. El-Bindary, Synthesis, structural characterization, molecular docking and DNA binding studies of copper complexes, *J. Mol. Liq.* 249 (2018) 533–545. <https://doi.org/10.1016/j.molliq.2017.11.072>
11. H.A. Kiwaan, T.M. Atwee, E.A. Azab, A.A. El-Bindary, Efficient photocatalytic degradation of Acid Red 57 using synthesized ZnO nanowires, *J. Chin. Chem. Soc.* 66 (2019) 89–98. [doi: 10.1002/jccs.201800092](https://doi.org/10.1002/jccs.201800092)
12. A.A. El-Bindary, N. Hassan, M.A. El-Afify, Synthesis and structural characterization of some divalent metal complexes: DNA binding and antitumor activity, *J. Mol. Liq.* 242 (2017) 213–228. <https://doi.org/10.1016/j.molliq.2017.07.009>
13. S. Brunauer, P.H. Emmett, E. Teller, Adsorption of gases in multimolecular layers, *J. Am. Chem. Soc.* 60 (1938) 309–319.
14. A.A. El-Bindary, S.M. El-Marsafy, A.A. El-Maddah, Enhancement of the photocatalytic activity of ZnO nanoparticles by silver doping for the degradation of AY99 contaminants, *Journal of Molecular Structure* 1191 (2019) 76–84. <https://doi.org/10.1016/j.molstruc.2019.04.064>
15. K.Z. Elwakeel, A.A. El-Bindary, A. Ismail, A.M. Morshidy, Magnetic chitosan grafted with polymerized thiourea for remazol brilliant blue R recovery: Effects of uptake conditions, *J. Dispers. Sci. Technol.* 38 (2017) 943–952. <http://dx.doi.org/10.1080/01932691.2016.1216436>
16. I. Langmuir, The constitution and fundamental properties of solids and liquids. II. Liquids, *J. Am. Chem. Soc.* 39 (1917) 1848–1906.
17. I. Langmuir, The adsorption of gases on plane surfaces of glass, mica and platinum, *J. Am. Chem. Soc.* 40 (1918) 1361–1403.
18. H. Freundlich, W. Heller, The adsorption of cis- and trans-azobenzene, *J. Am. Chem. Soc.* 61 (1939) 2228–2230.
19. M.M. Dubinin, E.D. Zaverina, L.V. Radushkevich, Sorption and structure of active carbons. I. Adsorption of organic vapors, *Zh. Fiz. Khim.* 21 (1947) 1351–1362.
20. M.J. Temkin, V. Pyzhev, Recent modifications to Langmuir isotherms, *Acta Physicochim. URSS* 12 (1940) 217–222.
21. S. Lagergren, Zur theorie der sogenannten adsorption gelöster stoffe, *Kunliga Svenska Vetenskapsakad, Handl.* 24 (1898) 1–39.
22. Y.S. Ho, G. McKay, Sorption of dye from aqueous solution by peat, *Chem. Eng. J.* 70(2) (1998) 115–124.
23. J. Zeldowitsch, Über den Mechanismus der katalytischen Oxydation von CO an MnO₂, *Acta Physicochim. URSS* 1 (1934) 364–449.

24. M.H. Dehghani, A. Dehghan, A. Najafpoor, Removing reactive red 120 and 196 using chitosan/zeolite composite from aqueous solutions: Kinetics, isotherms, and process optimization, *J. Ind. Eng. Chem.* 51 (2017) 185–195. <http://dx.doi.org/10.1016/j.jiec.2017.03.001>
25. Y. Zhang, G. Huang, C. An, X. Xin, X. Liu, M. Raman, Y. Yao, W. Wang, M. Doble, Transport of anionic azo dyes from aqueous solution to gemini surfactant-modified wheat bran: Synchrotron infrared, molecular interaction and adsorption studies, *Sci. Total Environ.* 595 (2017) 723–732. [doi: 10.1016/j.scitotenv.2017.04.031](https://doi.org/10.1016/j.scitotenv.2017.04.031)
26. R.S. Juang, F.C. Wu, R.L. Tseng, The ability of activated clay for the adsorption of dyes from aqueous solutions, *Environ. Technol.* 18(5) (1997) 525–531. <https://doi.org/10.1080/09593331808616568>
27. H. Nollet, M. Roels, P. Lutgen, P. Van der Meeren, W. Verstraete, Removal of PCBs from wastewater using fly ash, *Chemosphere* 53(6) (2003) 655–665. [DOI: 10.1016/S0045-6535\(03\)00517-4](https://doi.org/10.1016/S0045-6535(03)00517-4)
28. M.R. Fathi, A. Asfaram, A. Farhangi, Removal of direct red 23 from aqueous solution using corn stalks: isotherms, kinetics and thermodynamic studies, *Spectrochim. Acta A* 135 (2015) 364–372. [DOI:10.1016/j.saa.2014.07.008](https://doi.org/10.1016/j.saa.2014.07.008)
29. C. Prasad, S. Karlapudi, P. Venkateswarlu, I. Bahadur, S. Kumar, Green arbitrated synthesis of Fe₃O₄ magnetic nanoparticles with nanorod structure from pomegranate leaves and Congo red dye degradation studies for water treatment *J. Mol. Liq.* 240 (2017) 322–328. <https://doi.org/10.1016/j.molliq.2017.05.100>
30. J. Liu, H. Yu, Q. Liang, Y. Liu, J. Shen, Q. Bai, Preparation of polyhedral oligomeric silsesquioxane based cross-linked inorganic-organic nanohybrid as adsorbent for selective removal of acidic dyes from aqueous solution, *J. Colloid. Interf. Sci.* 497 (2017) 402–412. [doi: 10.1016/j.jcis.2017.03.028](https://doi.org/10.1016/j.jcis.2017.03.028)

(2019); <http://www.jmaterenvirosci.com>